



Detecting Topological Quantum Phase Transitions via the c -Function

Matteo Baggioli ^{1,*} and Dimitrios Giataganas ^{2,3,†}

¹*Instituto de Física Teórica UAM/CSIC, c/Nicolas Cabrera 13-15, Universidad Autónoma de Madrid, Cantoblanco, 28049 Madrid, Spain.*

²*Department of Physics, University of Athens, 15771 Athens, Greece.*

³*Physics Division, National Center for Theoretical Sciences, National Tsing-Hua University, Hsinchu, 30013, Taiwan.*

We propose the c -function as a new and accurate probe to detect the location of topological quantum critical points. As a direct application, we consider a holographic model which exhibits a topological quantum phase transition between a topologically trivial insulating phase and a gapless Weyl semimetal. The quantum critical point displays a strong Lifshitz-like anisotropy in the spatial directions and the quantum phase transition does not follow the standard Landau paradigm. The c -function robustly shows a global maximum at the quantum criticality and distinguishes with great accuracy the two separate zero temperature phases. We expect our proposal to be a general feature of quantum phase transitions and to be applicable beyond the holographic framework.

INTRODUCTION

Phase transitions are ubiquitous in nature and they provide one of the most elegant examples of *Universality* and a new window into the physics of strongly correlated quantum many-body systems [1]. Of exceptional interest are phase transitions happening at zero temperature – the *quantum phase transitions* [2] – which require a shift of paradigm within the condensed matter lore since they do not admit a simple Ginzburg-Landau description [3] and they are often not characterized by any spontaneous symmetry breaking pattern. A typical case is that of metal-insulator transitions [4].

Topological quantum phase transitions (TQPT) are a particularly challenging subclass; the most famous example being quantum hall systems, displaying exotic features such as fractional statistics and topological degeneracy [5, 6]. The chase for an “*order parameter*” or a local quantity able to pinpoint the location of the TQPT is a pressing and fundamental open question given the plethora of topological phases discovered in the recent years and their possible importance for technological developments such as quantum computing [7].

In recent years, there have been several attempts to find an efficient observable able to locate the TQPT from the nature of the quasiparticles [8], the (not Ising-like) critical exponents [9], the *dynamical topological order parameter* [10] to other quantum information quantities such as *fidelity* [11] and *topological entanglement entropy* [12, 13].

In this work, we propose a different and particularly effective way to detect TQPTs by considering the c -function of the system. We show that such quantity displays a neat and narrow signal at the location of the quantum critical point and it is therefore able to identify with precision the separation between the two topological

phases.

The c -function is a natural candidate to detect phase transitions. The re-organization of the degrees of freedom (*dofs*) along a transition is a key-feature to understand the two different phases involved. In relativistic theories, a clear measure for the number of effective degrees of freedom is indeed provided by the c -function, whose monotonicity along the renormalization group (RG) flow is guaranteed by c -theorems [14–21]. These theorems formalize the idea that the number of *dofs* diminishes monotonically flowing towards low energy and their validity is tightly connected with the existence of a null energy condition (NEC) [22]. At any fixed point, the c -function coincides with the *central charge* c of the system.

The proof of the c -theorems relies crucially on Lorentz invariance and the monotonicity of the c -function is not guaranteed if such set of symmetries is broken [23–26]. Additionally, when the rotational global symmetries are broken, as it happens in anisotropic Lifshitz-like fixed points, the c -function needs to be redefined appropriately. Such a c -function was introduced in [25], further studied in [27, 28], and it has already passed various non trivial tests within the holographic scenario. Therefore, we will use it here as a probe for the TQPT.

As a concrete scenario, we consider the holographic Weyl semimetal model introduced in [29, 30] (see [31] for more details). This setup realizes a quantum phase transition of topological nature between a Weyl semimetal and an insulating phase (see Fig.1). The topological distinction between the two phases is described by a topological invariant which has been computed in the context of probe fermions [32]. Related to this model there are several holographic studies [33–41].

More broadly, Weyl semimetals (WS) are new 3D materials whose band structure is characterized by singularity

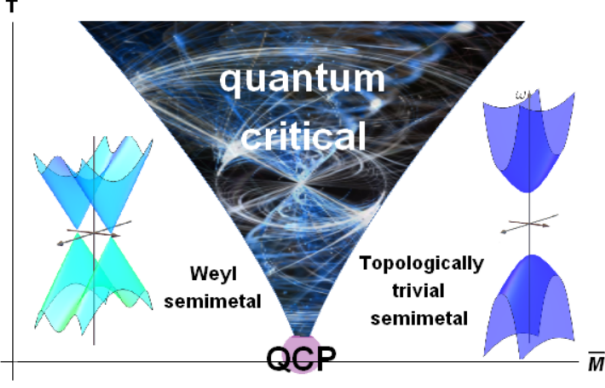


Figure 1. A sketch of the TQPT considered in this work. For our choice of parameters, the transition appears at a critical value $\bar{M}_c \sim 0.744$ between a topologically trivial gapped state and a Weyl semimetal phase.

points at which the two bands touch, producing linearly dispersing cones [42]. The low-energy description at those points displays emergent relativistic symmetry and it is described by chiral Weyl spinors always appearing in pairs [43]. WS exhibit exotic transport properties which are a direct consequence of quantum field theory anomalies [44]. To comprehend the fundamental dynamics of WS and the TQPT, it is sufficient to consider a simple weakly coupled field theory whose fermionic lagrangian reads [45]

$$\mathcal{L} = \bar{\Psi} \left(i \not{\partial} - e \not{A} - \gamma_5 \vec{\gamma} \cdot \vec{b} + M \right) \Psi, \quad (1)$$

where e is the EM coupling, γ_i the Dirac matrices, A is the electromagnetic potential, M a mass parameter and \vec{b} a vector which describes the separation in momentum space of the two Weyl cones. The system considered exhibits a spectrum which, as expected, depends on the dimensionless ratio $M/|\vec{b}|$. In the regime $M > |\vec{b}|$ the system is gapped and the effective fermionic excitations have an effective mass $M_{eff}^2 = M^2 - |\vec{b}|^2$, while in the opposite scenario, $M < |\vec{b}|$, the spectrum is characterized by band inversion and the fermions at the crossing points are massless and separated by the effective parameter $|\vec{b}_{eff}|^2 = b^2 - M^2$. Importantly, the axial anomaly implies an anomalous hall conductivity [46]:

$$\sigma_{AHE} = \frac{1}{(2\pi)^2} |\vec{b}_{eff}|, \quad (2)$$

which is non-zero only in the topological Weyl semimetal phase.

In this work, we examine the holographic Weyl semimetal model and we show that the c-function serves as a very efficient tool to diagnostic the location of the TQPT. More generally, it is natural to expect that this concept can apply beyond the realm of holography and could provide a new and fundamental tool for quantum phase transitions evading the standard Landau logic.

THE TOPOLOGICAL PHASE TRANSITION

Our holographic model is defined by the following 5-dimensional bulk action [30]:

$$\mathcal{S} = \int d^5x \sqrt{-g} \left[R + 12 - \frac{1}{4} F^2 - \frac{1}{4} F_5^2 - V(\Phi) - (D_\mu \Phi)^* (D_\mu \Phi) + \frac{\alpha}{3} \epsilon^{\mu\nu\rho\sigma\tau} A_\nu \left(F_{\nu\rho}^5 F_{\sigma\tau}^5 + 3 F_{\nu\rho} F_{\sigma\tau} \right) \right], \quad (3)$$

written in terms of a vector $U(1)_v$ field B_μ with field-strength $F \equiv dB$, an axial vector field A_μ with field-strength $F_5 \equiv dA$ and a complex scalar field Φ charged under the gauge symmetry $U(1)_v$. Moreover, the covariant derivative is defined as $D_\mu \Phi = \partial_\mu - iq A_\mu \Phi$, and the scalar potential is chosen to be $V(\Phi) = m^2 |\Phi|^2 + \frac{\lambda}{2} |\Phi|^4$. We use the following anisotropic, in the x_3 direction, ansatz for the various bulk fields

$$ds^2 = -f(r) dt^2 + \frac{dr^2}{f(r)} + g(r) (dx_1^2 + dx_2^2) + h(r) dx_3^2, \\ A = A_3(r) dx_3, \quad \Phi = \phi(r), \quad (4)$$

where $f(r)$, $g(r)$ and $h(r)$ depend solely on the radial coordinate r . We choose $m^2 = -3$ to fix the dimension of the scalar operator dual to the bulk field Φ to be $\Delta_\mathcal{O} = 3$. For this choice, the asymptotics of the gauge field and the bulk scalar are given by:

$$\lim_{r \rightarrow \infty} r \Phi = M, \quad \lim_{r \rightarrow \infty} A_3 = b, \quad (5)$$

where M and b are free parameters of the model, which play the same role as those in Eq.(1). Moreover, without loss of generality, we choose $\lambda = 1/10$ and $q = 1$.

The theory therefore is characterized by two dimensionless parameters taken as $\bar{T} \equiv T/b$ and $\bar{M} \equiv M/b$ and exhibits a quantum critical transition at $\bar{M}_c \sim 0.74$.

At zero temperature, our model admits three types of solutions – (I) for $\bar{M} > \bar{M}_c$: an insulating background, (II) for $\bar{M} = \bar{M}_c$: a critical background, and (III) for $\bar{M} < \bar{M}_c$ a semimetal background.

The full background of the RG flow, can be found only numerically and exhibits different IR fixed points depending on the dimensionless parameter \bar{M} . The near-horizon geometry of the topologically trivial gapped solution (I) is an AdS_5 domain-wall with $A_3(r) = a_1 r^{\beta_1}$, $\phi(r) = \sqrt{3/\lambda} + \phi_1 r^{\beta_2}$, where the exponents $\beta_{1,2}$ are functions of the parameters (m, λ, q) . In this regime (I), the near-horizon value of A_3 is always zero, and that of ϕ is $\sqrt{3/\lambda}$. At the quantum critical point (II), the solution is *exact* and the theory displays an anisotropic Lifshitz-like scaling parametrized by z , and induced by the source of the axial gauge field A_3 . The background can be expressed as

$$f(r) = f_0 r^2, \quad h(r) = h_0 r^{2/z}, \quad (6)$$

$$A_3(r) = r^{1/z}, \quad \phi(r) = \phi_0, \quad (7)$$

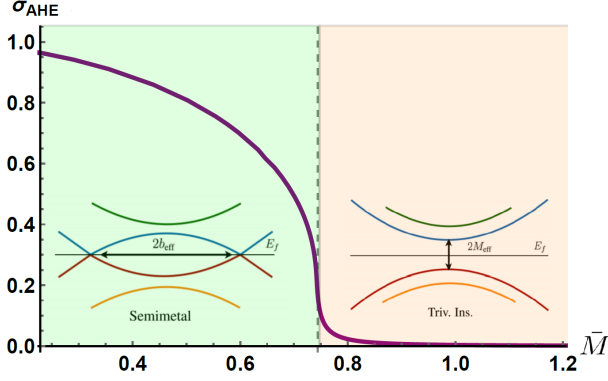


Figure 2. The anomalous conductivity at low temperature $\bar{T} = 0.005$ in function of the external parameter \bar{M} . The dashed line indicates the position of the quantum critical point $\bar{M}_c \sim 0.744$. The inset displays the topological band crossing which characterizes the semimetal phase. E_f is the Fermi energy of the system.

where all the parameters are fixed completely by the choice of (m, λ, q) . In particular, the anisotropic exponent is given by $z = -(m^2 + \lambda\phi_0^2 - 2q^2)/2q^2$ and takes a value around $z \simeq 2.46$ for our choice of parameters. Null Energy Conditions, the regularity of the solution and the thermodynamic stability generally imply that $z \geq 1$ [25, 47]. The near-horizon value of A_3 at criticality is always zero, whereas that of ϕ is finite equal to ϕ_0 . Finally, by reducing the parameter \bar{M} to values lower than the critical one, we enter in the semimetal phase (III) where the near-horizon geometry is simply AdS_5 with

$$A_3(r) = a_1 + \frac{c_1^2 \pi}{4r} e^{-\frac{2a_1}{r}}, \quad \phi(r) = \sqrt{\pi} \phi_1 \left(\frac{c_1}{r} \right)^{3/2} e^{-\frac{a_1}{r}}, \quad (8)$$

and the various constants depending on the parameters of the model. In this regime, the near horizon value of A_3 is finite, equal to a_1 ; however, $\phi(r_0)$ vanishes. To distinguish the two different phases, we consider the anomalous Hall conductivity depicted in Fig.2:

$$\sigma_{AHE} \sim A_3|_{\text{horizon}}. \quad (9)$$

The conductivity serves as a non-local order parameter for the TQPT, which vanishes in the topologically trivial insulating phase ($\bar{M} > \bar{M}_c$) and it becomes finite in the Weyl semimetal phase. Interesting, this "order parameter" does not obey a mean-field theory description but it rather follows a different scaling:

$$\sigma_{AHE} \sim (\bar{M}_c - \bar{M})^{0.21}, \quad (10)$$

which is shown for our lowest temperature in Fig.2.

In our scenario, the anisotropy is a characteristic property of the quantum critical point defining the corresponding class of universality, while away of criticality isotropy

is always re-emerging. This is a crucial difference with respect to the confinement/deconfinement phase transitions in Einstein-Dilaton-Axion theories [48] which contain a finite degree of anisotropy that remains invariant along the different phases.

THE C-FUNCTION FOR LIFSHITZ-LIKE SYSTEMS

For the sake of introducing the notion of the anisotropic c-function, let us temporarily consider an arbitrary dimensional spacetime in which the d -dimensional spatial subspace can be decomposed in a transverse and parallel sets with respective dimensions d_1, d_2 , ($d_1 + d_2 = d$), enjoying different scalings:

$$[||] = L^{n_1}, \quad [\perp] = L^{n_2}, \quad (11)$$

and therefore breaking the rotational $SO(d)$ invariance to $SO(d_1) \times SO(d_2)$. The natural proposal for the c-function of these theories is given by [25]

$$c_{||} := \beta_{||} \frac{l_{||}^{d_{||}-1}}{H_{||}^{d_{||}-1} H_{\perp}^{d_2}} \frac{\partial S_{||}}{\partial \ln l_{||}}, \quad c_{\perp} := \beta_{\perp} \frac{l_{\perp}^{d_{\perp}-1}}{H_{||}^{d_1} H_{\perp}^{d_2-1}} \frac{\partial S_{\perp}}{\partial \ln l_{\perp}}, \quad (12)$$

where $S_{||} (S_{\perp})$ is the entanglement of the slab geometry with length $l_{||} (l_{\perp})$ along one of the spatial $||, (\perp)$ dimensions and H corresponds to the UV cut-offs. The $d_{||}$ and d_{\perp} are the effective dimensions:

$$d_{||} := d_1 + d_2 \frac{n_2}{n_1}, \quad d_{\perp} := d_1 \frac{n_1}{n_2} + d_2, \quad (13)$$

of the two rotational invariant spatial planes of dimensions d_1 and d_2 , where the initial isotropy has been broken to. The parameters $\beta_{||, \perp}$ are just dimensionless normalization constants. The entangling surface in $(||, \perp)$ directions is computed holographically with the usual strategy on anisotropic probes introduced in [49]. When the c-function is computed at a certain fixed point, the effective dimensions are identified with the corresponding scaling exponents. Importantly, the above definition Eq.(12) reduces to the conformal and isotropic c-function [17, 19, 20] when the symmetries (in this case isotropy) are restored.

UNCOVERING THE QUANTUM CRITICAL POINT

To uncover the criticality of the theory, we firstly obtain the numerical background of Eq.(4) for $\bar{M} \in [0, 4]$, while keeping fixed the dimensionless temperature \bar{T} . We are primarily interested in extremely low temperatures ($\bar{T} \simeq 0.005$). Nevertheless, we have directly checked that similar results are obtained for slightly larger values ($\bar{T} = 0.05, 0.1$).

In order to locate the quantum critical point, we compute the c-function corresponding to an entangling surface with fixed large enough boundary length to extend away from the boundary into the bulk. This type of entangling region probes the deep IR (i.e. the bulk region near the black hole horizon) and provides good accuracy on locating the phase transitions. The c-function defined in (12) has the advantage of being valid and well-defined even for anisotropic IR phases. Exploiting this feature, we are able to compute it across the full phase diagram (\bar{M}, \bar{T}) . Notice that this would have been impossible by using of the isotropic c-function, because the quantum critical point exhibits a strong anisotropic character.

Practically, the external parameter \bar{M} is dialed in a range able to cover the three different phases of the theory: trivial insulator ($\bar{M} > 0.744$), critical point ($\bar{M} \sim 0.744$) and Weyl semimetal ($\bar{M} < 0.744$) (see Figures 1 and 2). The c-function develops a clear pattern. As we approach the quantum critical point, it increases and it reaches a maximum exactly at the quantum critical point with the Lifshitz-like symmetry. In this sense, the c-function acts as a very accurate probe to locate the topological quantum critical point.

We show our main results in Fig.3. Both c-functions detect very accurately the position of the anisotropic quantum critical point. By increasing the size of the entangling surface at the boundary, the precision improves and the matching is almost exact (see bottom panel of Fig.3). Practically, a larger entangling surface implies that the corresponding surface probes deeper the IR structure of the theory. Given the quantum critical ($T = 0$) nature of the phase transition, it is then very natural that the precision in locating it becomes better and better in this way. In other words, the precision of the probe grows with the size of the entangling surface.

Before concluding, few comments are in order. The c-function defined in (12) contains accurate information to signal the phase transition in its terms. In fact, the information of the phase transition is included in the effective dimensions d_{\parallel} and d_{\perp} since the critical point has Lifshitz-scaling anisotropy, in contrast to the AdS phases. Information of the phase transition is also included in the entangling surface itself. We show the behaviour of the effective dimensions and the EE derivatives¹ in function of \bar{M} in Fig.4. The first observable over-estimates the location of the QCP, at least for our chosen values², while the second under-estimates it. Interestingly, the exact

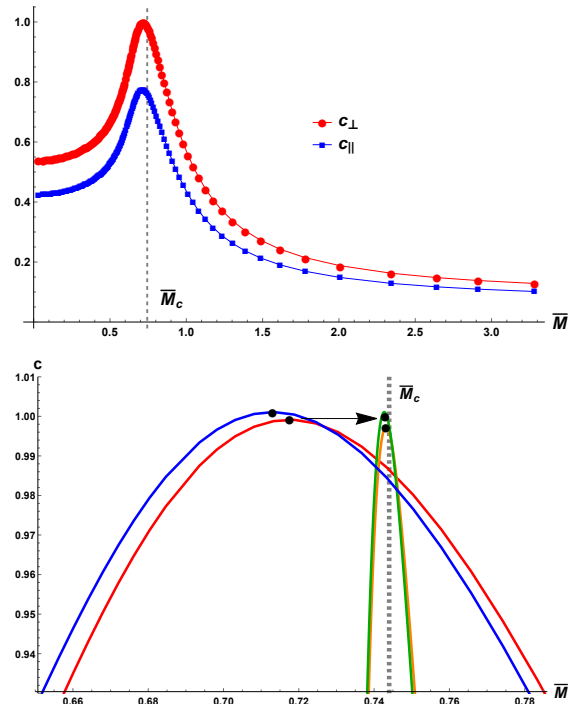


Figure 3. **Top:** The parallel and transverse c-functions at $\bar{T} = 0.005$ in function of the external parameter \bar{M} . The dashed line indicates the position of the quantum critical point, $\bar{M}_c \sim 0.744$. **Bottom:** The same c-functions (blue, red) for a larger entangling region (orange, green) and the dynamics of the maxima (black dots). The arrows indicate the motion of the maxima increasing the size L of the entangling region and the dashed line the quantum critical point. In both panels the normalizations are arbitrary.

combination of the two, which appears in (12), is the one that pinpoints the precise position of the quantum critical point with the greatest accuracy. Let us also notice that, considering large regions at the boundary, the entanglement entropy is expected to approach the thermal entropy of the system, as it usually happens in the thermal theories e.g. [52]. This may lead to thermal contributions on the computed entanglement entropy, which however are not affecting the ability of the c-function to locate the probe.

DISCUSSION

In this work we have considered a holographic model exhibiting a topological quantum phase transition (TQPT). The quantum critical point, which is related to the transition between a topologically trivial insulator and a gapless

¹ Different EE derivatives have been already considered in [50, 51] for certain holographic Q-lattices model.

² Interestingly, the parallel effective dimension displays a minimum

at the QCP instead of a maximum. This is similar to the behaviours of the conductivities, viscosities and butterfly velocities [39].

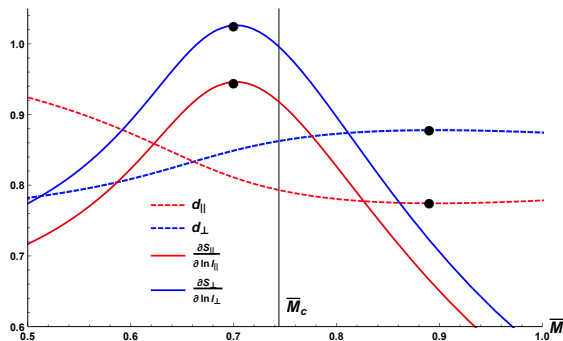


Figure 4. The effective dimensions $d_{\parallel,\perp}$ and the EE derivatives $\partial S_{\parallel,\perp} / \partial \ln l_{\parallel,\perp}$ in function of the external parameter \bar{M} . The black dots indicate the position of the maxima for these observables while the vertical line the location of the QCP. In both panels the normalizations are arbitrary.

Weyl semimetal, displays a Lifshitz-like anisotropic critical point and critical scalings not compatible with the standard Landau paradigm. We have shown that the anisotropic c-function attains a universal maximum at the location of the quantum critical point and as such it serves as a very accurate and efficient probe to detect the TQPT.

More broadly, we propose that the generalized c-function might have a comprehensive and fundamental role in the context of “exotic” (not classical/thermal) phase transitions for which symmetry breaking arguments à la Landau are of no help. Our conclusions are expected to have a universal character which can be confirmed with direct computations outside the holographic framework.

ACKNOWLEDGMENTS

We would like to thank C-S Chu, S.Cremonini, J.P. Derendinger, M.Flory, S.Grieninger, L.Li, K.Landsteiner, B.Padhi, Y.Liu, and Y.W.Sun for useful discussions and suggestions. M.B. acknowledges the support of the Spanish MINECO’s “Centro de Excelencia Severo Ochoa” Programme under grant SEV-2012-0249. D.G. research has been funded by the Hellenic Foundation for Research and Innovation (HFRI) and the General Secretariat for Research and Technology (GSRT), under grant agreement No 2344.

* matteo.baggioli@uam.es

† dgiataganas@phys.uoa.gr

- [1] X. Wen, Quantum Field Theory of Many-Body Systems: From the Origin of Sound to an Origin of Light and Electrons (OUP Oxford, 2004).
- [2] S. Sachdev, [Quantum Phase Transitions](#) (Cambridge University Press, 2011).

- [3] L. D. Landau and V. L. Ginzburg, *Zh. Eksp. Teor. Fiz.* **20**, 1064 (1950).
- [4] M. Imada, A. Fujimori, and Y. Tokura, *Rev. Mod. Phys.* **70**, 1039 (1998).
- [5] D. C. Tsui, H. L. Stormer, and A. C. Gossard, *Phys. Rev. Lett.* **48**, 1559 (1982).
- [6] R. B. Laughlin, *Phys. Rev. Lett.* **50**, 1395 (1983).
- [7] A. Kitaev and C. Laumann, Exact methods in low-dimensional statistical physics and quantum computing,” Lecture Notes of the Les Houches Summer School , 101 (2009).
- [8] S. Manna, N. S. Srivatsa, J. S. Wildeboer, and A. E. Nielsen, arXiv: Strongly Correlated Electrons (2019).
- [9] Y. Ran and X.-G. Wen, *Phys. Rev. Lett.* **96**, 026802 (2006).
- [10] X.-Y. Xu, Q.-Q. Wang, M. Heyl, J. C. Budich, W.-W. Pan, Z. Chen, M. Jan, K. Sun, J.-S. Xu, Y.-J. Han, C.-F. Li, and G.-C. Guo, *Light: Science & Applications* **9**, 7 (2020).
- [11] D. F. Abasto, A. Hamma, and P. Zanardi, *Phys. Rev. A* **78**, 010301 (2008).
- [12] A. Kitaev and J. Preskill, *Phys. Rev. Lett.* **96**, 110404 (2006).
- [13] M. Levin and X.-G. Wen, *Phys. Rev. Lett.* **96**, 110405 (2006).
- [14] A. Zamolodchikov, *JETP Lett.* **43**, 730 (1986).
- [15] J. L. Cardy, *Phys. Lett. B* **215**, 749 (1988).
- [16] Z. Komargodski and A. Schwimmer, *JHEP* **12**, 099 (2011), [arXiv:1107.3987 \[hep-th\]](#).
- [17] S. Ryu and T. Takayanagi, *JHEP* **08**, 045 (2006), [arXiv:hep-th/0605073](#).
- [18] R. C. Myers and A. Sinha, *JHEP* **01**, 125 (2011), [arXiv:1011.5819 \[hep-th\]](#).
- [19] H. Casini and M. Huerta, *Phys. Lett. B* **600**, 142 (2004), [arXiv:hep-th/0405111](#).
- [20] H. Casini and M. Huerta, *J. Phys. A* **40**, 7031 (2007), [arXiv:cond-mat/0610375](#).
- [21] R. C. Myers and A. Sinha, *Phys. Rev. D* **82**, 046006 (2010), [arXiv:1006.1263 \[hep-th\]](#).
- [22] R. C. Myers and A. Singh, *JHEP* **04**, 122 (2012), [arXiv:1202.2068 \[hep-th\]](#).
- [23] B. Swingle, *J. Stat. Mech.* **1410**, P10041 (2014), [arXiv:1307.8117 \[cond-mat.stat-mech\]](#).
- [24] S. Cremonini and X. Dong, *Phys. Rev. D* **89**, 065041 (2014), [arXiv:1311.3307 \[hep-th\]](#).
- [25] C.-S. Chu and D. Giataganas, *Phys. Rev. D* **101**, 046007 (2020), [arXiv:1906.09620 \[hep-th\]](#).
- [26] S. Cremonini, L. Li, K. Ritchie, and Y. Tang, (2020), [arXiv:2006.10780 \[hep-th\]](#).
- [27] I. Y. Aref’eva, A. Patrushev, and P. Slepov, (2020), [arXiv:2003.05847 \[hep-th\]](#).
- [28] C. Hoyos, N. Jokela, J. M. Penín, and A. V. Ramallo, *JHEP* **04**, 062 (2020), [arXiv:2001.08218 \[hep-th\]](#).
- [29] K. Landsteiner and Y. Liu, *Physics Letters B* **753**, 453 (2016).
- [30] K. Landsteiner, Y. Liu, and Y.-W. Sun, *Phys. Rev. Lett.* **116**, 081602 (2016).
- [31] K. Landsteiner, Y. Liu, and Y.-W. Sun, *Sci. China Phys. Mech. Astron.* **63**, 250001 (2020), [arXiv:1911.07978 \[hep-th\]](#).
- [32] Y. Liu and Y.-W. Sun, *JHEP* **10**, 189 (2018), [arXiv:1809.00513 \[hep-th\]](#).
- [33] X. Ji, Y. Liu, and X.-M. Wu, *Phys. Rev. D* **100**, 126013 (2019), [arXiv:1904.08058 \[hep-th\]](#).

- [34] Y. Liu and J. Zhao, *JHEP* **12**, 124 (2018), [arXiv:1809.08601 \[hep-th\]](#).
- [35] Y. Liu and Y.-W. Sun, *JHEP* **12**, 072 (2018), [arXiv:1801.09357 \[hep-th\]](#).
- [36] K. Landsteiner, Y. Liu, and Y.-W. Sun, *Phys. Rev. Lett.* **117**, 081604 (2016), [arXiv:1604.01346 \[hep-th\]](#).
- [37] G. Grignani, A. Marini, F. Pena-Benitez, and S. Speziali, *JHEP* **03**, 125 (2017), [arXiv:1612.00486 \[cond-mat.str-el\]](#).
- [38] C. Copetti, J. Fernández-Pendás, and K. Landsteiner, *JHEP* **02**, 138 (2017), [arXiv:1611.08125 \[hep-th\]](#).
- [39] M. Baggioli, B. Padhi, P. W. Phillips, and C. Setty, *JHEP* **07**, 049 (2018), [arXiv:1805.01470 \[hep-th\]](#).
- [40] M. Ammon, M. Baggioli, A. Jiménez-Alba, and S. Moeckel, *JHEP* **04**, 068 (2018), [arXiv:1802.08650 \[hep-th\]](#).
- [41] M. Ammon, M. Heinrich, A. Jiménez-Alba, and S. Moeckel, *Phys. Rev. Lett.* **118**, 201601 (2017), [arXiv:1612.00836 \[hep-th\]](#).
- [42] O. Vafek and A. Vishwanath, *Annual Review of Condensed Matter Physics* **5**, 83 (2014), <https://doi.org/10.1146/annurev-conmatphys-031113-133841>.
- [43] H. Nielsen and M. Ninomiya, *Physics Letters B* **130**, 389 (1983).
- [44] K. Landsteiner, *Acta Phys. Polon. B* **47**, 2617 (2016), [arXiv:1610.04413 \[hep-th\]](#).
- [45] D. Colladay and V. Kostelecky, *Phys. Rev. D* **58**, 116002 (1998), [arXiv:hep-ph/9809521](#).
- [46] F. D. M. Haldane, *Phys. Rev. Lett.* **93**, 206602 (2004).
- [47] C. Hoyos and P. Koroteev, *Phys. Rev. D* **82**, 084002 (2010), [Erratum: *Phys. Rev. D* **82**, 109905 (2010)], [arXiv:1007.1428 \[hep-th\]](#).
- [48] D. Giataganas, U. Gürsoy, and J. F. Pedraza, *Phys. Rev. Lett.* **121**, 121601 (2018), [arXiv:1708.05691 \[hep-th\]](#).
- [49] D. Giataganas, *JHEP* **07**, 031 (2012), [arXiv:1202.4436 \[hep-th\]](#).
- [50] Y. Ling, P. Liu, and J.-P. Wu, *Phys. Rev. D* **93**, 126004 (2016), [arXiv:1604.04857 \[hep-th\]](#).
- [51] Y. Ling, P. Liu, C. Niu, J.-P. Wu, and Z.-Y. Xian, *JHEP* **04**, 114 (2016), [arXiv:1502.03661 \[hep-th\]](#).
- [52] D. Giataganas and N. Tetradis, *Phys. Lett. B* **796**, 88 (2019), [arXiv:1904.13119 \[hep-th\]](#).

HOLOGRAPHIC BACKGROUND SOLUTION

Plugging our background ansatz (4) to the bulk action (3), we obtain the following equations of motion:

$$f'' + \frac{h'}{2h} f' - f \left(\frac{g''}{g} + \frac{g' h'}{2gh} \right) = 0, \quad (14)$$

$$\frac{f''}{2f} + \frac{g''}{g} + \frac{g' f'}{g f} - \frac{g'^2}{4g^2} - \frac{A_3'^2}{4h} + \frac{1}{2} \phi'^2 + \frac{m^2 \phi^2}{2f} - \frac{q^2 A_3^2 \phi^2}{2hf} + \frac{\lambda \phi^4}{4f} - \frac{6}{f} = 0, \quad (15)$$

$$\frac{1}{2} \phi'^2 + \frac{A_3'^2}{4h} - \left(\frac{g'}{2gf} + \frac{h'}{4hf} \right) f' - \frac{g' h'}{2gh} - \frac{g'^2}{4g^2} - \left(m^2 + \frac{q^2 A_3^2}{h} + \frac{\lambda \phi^2}{2} \right) \frac{\phi^2}{2f} + \frac{6}{f} = 0, \quad (16)$$

$$\phi'' + \phi' \left(\frac{g'}{g} + \frac{h'}{2h} + \frac{f'}{f} \right) - \frac{\lambda \phi^3}{f} - \left(\frac{q^2 A_3^2}{hf} + \frac{m^2}{f} \right) \phi = 0, \quad (17)$$

$$A_3'' + A_3' \left(\frac{g'}{g} - \frac{h'}{2h} + \frac{f'}{f} \right) - \frac{2q^2 A_3 \phi^2}{f} = 0. \quad (18)$$

At the UV boundary ($r = \infty$) the asymptotic expansion of the bulk fields is given by:

$$f = r^2 + \dots, \quad g = r^2 + \dots, \quad h = r^2 + \dots, \quad A_3 = b + \dots, \quad \phi = \frac{M}{r} + \dots \quad (19)$$

Our theory has the following three scaling symmetries

$$(x_1, x_2) \rightarrow a(x_1, x_2), \quad g \rightarrow ga^{-2}; \quad x_3 \rightarrow ax_3, \quad h \rightarrow a^{-2}h, \quad A_3 \rightarrow A_3 a^{-1} \quad (20)$$

$$r \rightarrow ar, \quad (t, x_1, x_2, x_3) \rightarrow (t, x_1, x_2, x_3)/a, \quad (f, g, h) \rightarrow a^2(f, g, h), \quad A_3 \rightarrow aA_3, \quad (21)$$

which are used to rescale the coefficients of the three different metric functions (f, g, h) at the boundary to unity. This is why the boundary field theory depends only on the parameters, T, b, M which can be reorganized into two dimensionless quantities $\bar{T} \equiv T/b$ and $\bar{M} \equiv M/b$.

Approaching the black-brane horizon (r_h), the expansion for the bulk fields can be written as

$$f \simeq 4\pi T(r - r_h) + f_2(r - r_h), \quad g \simeq g_1 + g_2(r - r_h), \quad h \simeq h_1 + h_2(r - r_h), \quad (22)$$

$$A_3 \simeq A_3^{(1)} + A_3^{(2)}(r - r_h), \quad r\phi \simeq \phi_1 + \phi_2(r - r_h).$$

$A_3^{(1)}$ and ϕ_1 are the only free parameters, controlled by the boundary data \bar{T} and \bar{M} . In summary, we can reduce the number of the independent horizon parameters $(T, r_h, g_1, h_1, A_3^{(1)}, \phi_1)$ to $(T, A_3^{(1)}, \phi_1)$ using the above scaling symmetries. At the conformal boundary, these parameters can be mapped into the triplet (T, M, b) . Following this procedure, we obtain numerically our background using the shooting method with respects to parameters \bar{T} and \bar{M} .